TB09

19th International Symposium of Ballistics, 7–11 May 2001, Interlaken, Switzerland

SIZE SCALING IN BALLISTIC LIMIT VELOCITIES FOR SMALL FRAGMENTS PERFORATING THIN PLATES

E. J. O'Connor[1], J.D. Yatteau[2], P.T. Dzwilewski[2], S.R. Ford[3] and J.W. Black[1]

[1]Naval Surface Warfare Center Dahlgren Division, Dahlgren, VA 22448, U.S.A.
[2]Applied Research Associates, Littleton, CO 80123, U.S.A.
[3]Denver Research Institute, University of Denver, Denver, CO 80208, U.S.A.

Ballistic limit velocity data for steel cylinders perforating thin steel and aluminum plates indicate that ballistic limit velocities, for geometrically similar impacts, increase with decreasing fragment size below about 40 grains. This paper presents the results of recent ballistic limit velocity tests to confirm the size effect and the results of numerical simulations to determine if the CTH wave code with currently available material models can replicate the test results. The experiments involved steel spheres ranging in size from 12.7 mm down to 1.6 mm impacting aluminum plates with a normalized thickness, T/D, of 0.5. The current results confirm a size effect for the spheres, but it is not as strong as indicated by the cylinder data. The CTH numerical simulations reveal that the strain rate dependencies in the Johnson-Cook strength and fracture models for aluminum result in a predicted size effect for the spheres which is much smaller than that indicated by the current tests.

BACKGROUND

Recent comparisons between predictions from the FATEPEN penetration computer code and penetration test results for compact cylindrical fragments weighing between 1 and 10 grains revealed that the model generally over-predicted post-perforation residual velocities for these very small fragments by 10–20% [1]. Further analysis indicated that the residual velocity prediction errors derived primarily from under-predicting the ballistic limit velocities for these small fragments. The ballistic limit velocity, V_{50}, is the impact speed at which a particular penetrator has a 50% probability of perforating a particular target and is determined experimentally by performing a prescribed series of ballistic impact tests designed to bracket the minimum perforation velocity.

The FATEPEN ballistic limit velocity model derives in part from ballistic limit velocity test data for compact (L/D=1) cylindrical steel Fragment Simulating Projectiles (FSP's) impacting a variety of metallic and non-metallic plates at various impact obliquities [2]. The V_{50} formulas correlate these data as functions of the normalized plate thick-

ness, T/D, the slenderness ratio, L/D, of the cylinder, and the impact obliquity. This functional dependence follows from the hypothesis that the ballistic limit velocity for a particular penetrator and plate corresponds to a specific limit energy (i.e., impact energy per unit volume of target material). As such, the current V_{50} model presumes that geometric similitude applies in the sense that the magnitude of V_{50} does not depend on the absolute size of the penetrator and target but only on the relative target thickness (T/D) and penetrator shape (L/D). This formulation does not recognize any time or rate dependencies in either the penetrator or target strength and failure characteristics.

Mascianica's ballistic limit velocity data compilation for steel and aluminum plates includes data for FSP's weighing from 1.35 to 830 grains [2]. A comparison of V50 values for the same T/D across fragment sizes revealed a size effect wherein the ballistic limit velocities of the L/D=1, steel cylinders impacting steel or aluminum plates (presumably end-on impacts) with a fixed normalized thickness (T/D) increase with decreasing fragment weights below about 40 grains. The corresponding ballistic limit velocities for the larger fragments were found to decrease only slightly with increasing fragment size from 40 to 830 grains. Before modifying the FATEPEN formulas, it was decided to experimentally and computationally confirm the size effect because of uncertainties in the impact orientations associated with the smaller FSP V_{50} values.

BALLISTIC LIMIT VELOCITY TESTS

To avoid difficulties in achieving (and measuring) consistent impact orientations for very small cylinders, steel spheres were selected to confirm the ballistic limit velocity size effect. Stainless steel spheres (SAE/AISI 316) with diameters of 1.59, 3.18, 6.36, 9.53 and 12.7 mm (weights = 0.26, 2.0, 16.3, 55.9 and 131.8 grains) were impacted against 2024-T3 aluminum plates with thicknesses of 0.81, 1.58, 3.18, 4.78 and 6.25 mm, respectively. The resulting normalized plate thicknesses, T/D, ranged from 0.49 to 0.51. The hardnesses of the spheres ranged from Rc 25-39. The average plate hardnesses were measured at BHN 130, 144, 152, 110, and 152 in order of average increasing plate thickness (values converted from Rockwell K). The higher values are well above the expected nominal hardness of BHN 120 for 2024-T3 and additional hardness tests are planned using a Brinell hardness tester to confirm the results.

Test measurements included impact and residual velocity by means of two pairs of orthogonal flash X-rays. To aid in determination of the ballistic limit velocities, the target plates were mounted in a lightweight (16 lbs.) ballistic pendulum to record the impact or penetration impulse transmitted to the targets. The post-impact penetrators and target debris were soft recovered in polyglycol.

NUMERICAL SIMULATIONS

The Eulerian Finite Difference wave code CTH [4] was used to simulate the 1.59 mm and 12.7 mm steel sphere impact tests to determine if the current material models could replicate the test results and to gain further insight into the source of observed scaling effects. Both calculations used the Johnson-Cook strength and fracture models. The published values for the material dependent parameters in the model are listed in Table 1 for the steel spheres and aluminum plates. It is noted that the A and B coefficients for the aluminum plates were increased by 25% for the simulations to reflect the higher than published average hardness values measured for the plates.

Table 1: Constants for Johnson-Cook Srength and Fracture Models [4]

Material	A ($dynes/cm^2$)	B ($dynes/cm^2$)	n	C	m
2024 Aluminum (Published Values)	2.65×10^9	4.26×10^9	0.34	0.015	1.0
2024 Aluminum (Used in Simulations)	3.31×10^9	5.33×10^9	0.34	0.015	1.0
4340 Steel	7.92×10^9	5.10×10^9	0.26	0.014	1.03
Material	**D_1**	**D_2**	**D_3**	**D_4**	**D_5**
2024 Aluminum	0.13	0.13	-1.5	0.011	0.0
4340 Steel	-0.80	2.1	-0.5	0.002	0.61

The size scale factor between the 1.59 mm and 12.7 mm spheres is 8. Assuming that the strains for these geometrically similar impacts will be identical, the strain rates for the 1.59 mm simulations can be expected to be about 8 times that for the 12.7 mm simulations due to the shorter penetration time scale. The yield strength for the aluminum will increase by only 3%, and the strain to failure will increase by only 2% for the eight-fold decrease in scale.

TEST RESULTS

Fig. 1 contains close-up views of sectioned plates for impact speeds just below and just above the ballistic limit velocity for each of the stainless steel sphere sizes. The post-perforation spheres and plate plugs corresponding to the impacts above the V_{50} values are shown below the corresponding sectioned plates. It can be seen that the spheres perforated with no measurable deformation. At the impact speeds just below the V_{50}, the spheres imbedded and rebounded from the front surface producing a polished hemispherical crater, and they also ejected a plug very nearly identical to those shown in Fig. 1 for the impact speeds just above the V_{50}. The thickness of the plate plugs nearly match the thickness of the plates. In general, the macroscopic damage characteristics across the 8-fold size variation are quite similar. The only apparent size effect in Fig. 1 is that the diameter of the plate plugs appear to approach the diameter of spheres as sphere diameter decrea-

ses. The ballistic limit velocity test results are plotted in the penetration outcome graph in Fig. 2, and the V_{50} values for each sphere size are also tabulated in Fig. 1. The current sphere ballistic limit velocities normalized by the ballistic limit velocity for the 12.7 mm sphere are plotted in Fig. 3 where they are compared with similar normalized values for the cylindrical FSP's. The results in Figs. 2 and 3 confirm a clear size effect on ballistic limit velocity for the spheres, albeit a weaker one than that indicated by the FSP data in Fig. 3. An analysis balancing the shear work of plate plugging with pre-impact kinetic energy indicates that the observed growth in the plate plug diameter to sphere diameter could easily account for the observed increases in V_{50}.

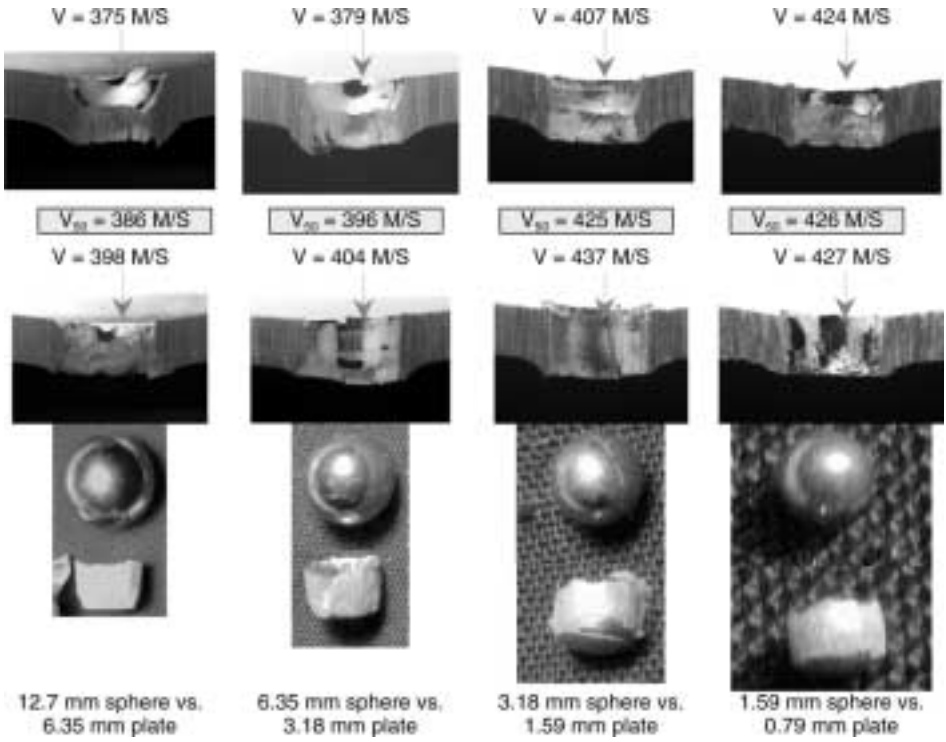

Figure 1: Sectioned plates and post-penetration spheres and plate plugs for stainless steel spheres impacting 2024-T3 aluminium plates at speeds slightly above (top) and below (bottom) the ballistic limit velocity, V_{50}. (note: images have been magnified to the apparent size to facilitate the discernment of size effects in the damage morphology.)

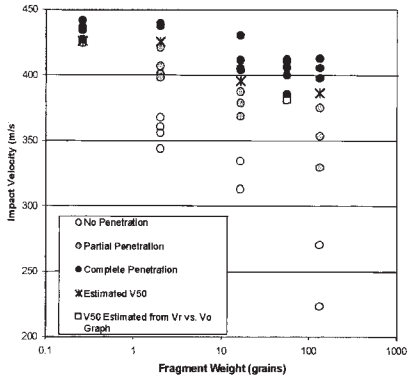

Figure 2: Ballistic limit velocity test results vs. fragment size, stainless steel spheres vs. 2024-T3 aluminium plates (T/D =0.5)

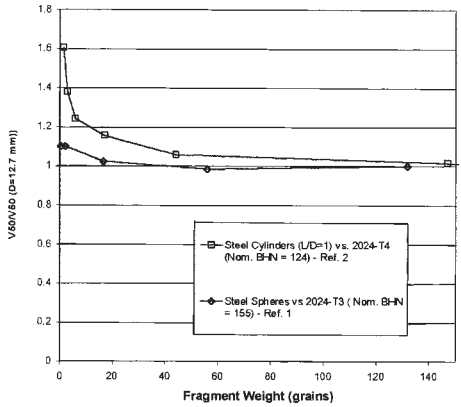

Figure 3: Ballistic limit velocity size effect for steel cylinders and spheres vs. aluminium plates (T/D=0.5)

NUMERICAL SIMULATIONS RESULTS

Fig. 4 contains CTH simulation results in the form of split images of the 12.7 and 1.59 mm spheres at the same scaled time. The initial velocity was 386 m/s (the experimentally determined value of V_{50} for the 12.7 mm sphere). It can be seen that the two simulations are in close agreement with regard to penetration depth and plate plug formation at the scaled times. Comparison with Fig. 1 shows that the simulation results exhibit many similarities to the recovered test specimens. However, there is no discernable predicted growth in the plate plug diameter with the decrease in size scale. The graphs in Fig. 5 compare the strain rates (in the plates) and sphere velocity time histories for these simulations. The Lagrange tracer data were recorded at the midpoint of the plate, one-half projectile radius from the central axis, where shear banding is most likely to occur and at the center of the sphere. The time scale for the smaller sphere results was expanded by a factor of 8 to facilitate comparisons at the same relative penetration depths in the two plates. As anticipated, the equivalent plastic strain rate of the larger plate is 1/8 that of the smaller. The predicted residual velocities for the 12.7 mm and 1.59 mm spheres were determined to be 113 m/s and 108 m/s, respectively. These values are consistent with the predicted strain rate differences and our initial expectations regarding the relatively weak influence of strain rate effects on the penetration results.

The CTH residual velocity predictions are plotted in Fig 6 where they are compared with the test results for the two spheres and with the following analytical model for penetration without mass loss [5]

$$V_r = \frac{\left(V_o^2 - V_{50}^2\right)^{1/2}}{1 + m/M} \tag{1}$$

where V_r is the residual velocity, V_o is the impact velocity, V_{50} is the ballistic limit velocity, M is the penetrator mass, and m is the intact plate plug mass.

The analytical predictions presume that the plate plug mass (m) is equal to the plug mass measured in the tests, and the values of V_{50} are measured values (Fig 1). The analytical model predictions provide a rational method to estimate the expected differences in CTH V50 predictions corresponding to the CTH V_r predictions. The V_{50} test results reveal a 10% increase in the ballistic limit velocity for the smallest sphere (1.59 mm). The estimated increase in the V_{50} value for the 1.59 mm sphere based on the CTH V_r results and Equation (1) is only about 1 % or 1/10 the observed size effect.

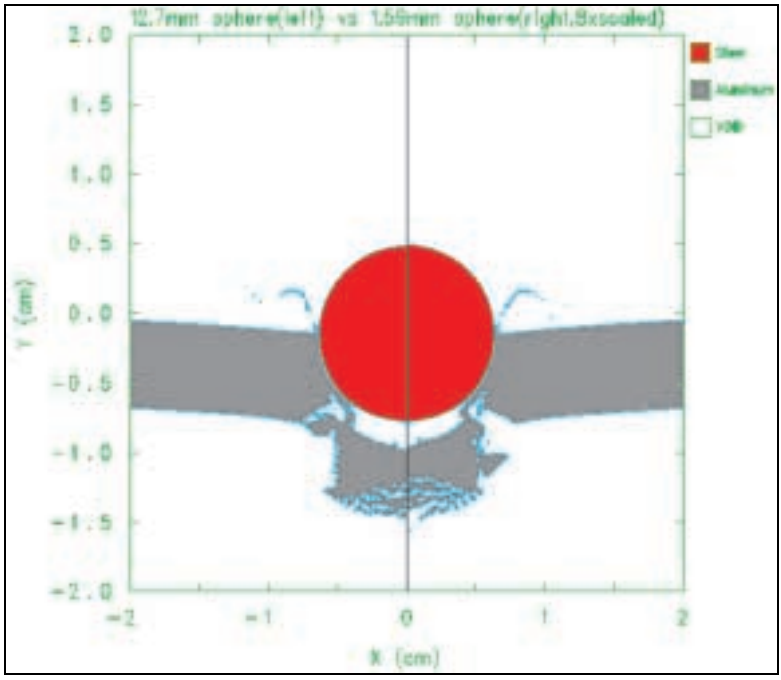

Figure 4: CTH numerical simulation results for the 12.7 mm sphere at 30 μ-sec (left) and 1.59 mm sphere at 3.75 μ-sec (right) impacting aluminium plates (T/D386 m/s. All dimensions of the 1.59 mm sphere and plate multiplied by a factor of eight to facilitate direct comparisons.

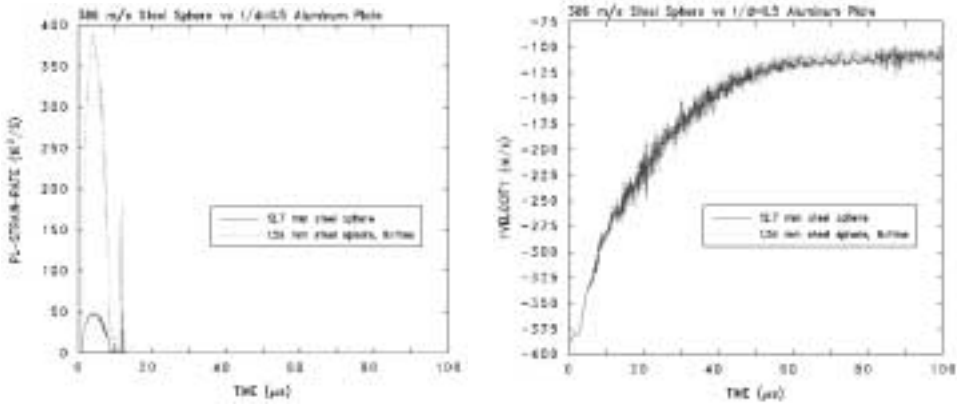

Figure 5: CTH time history plots of equivalent plastic strain rate in plate (left) and sphere velocity (right). Values of time for 1.59 mm sphere multiplied by a factor of eight.

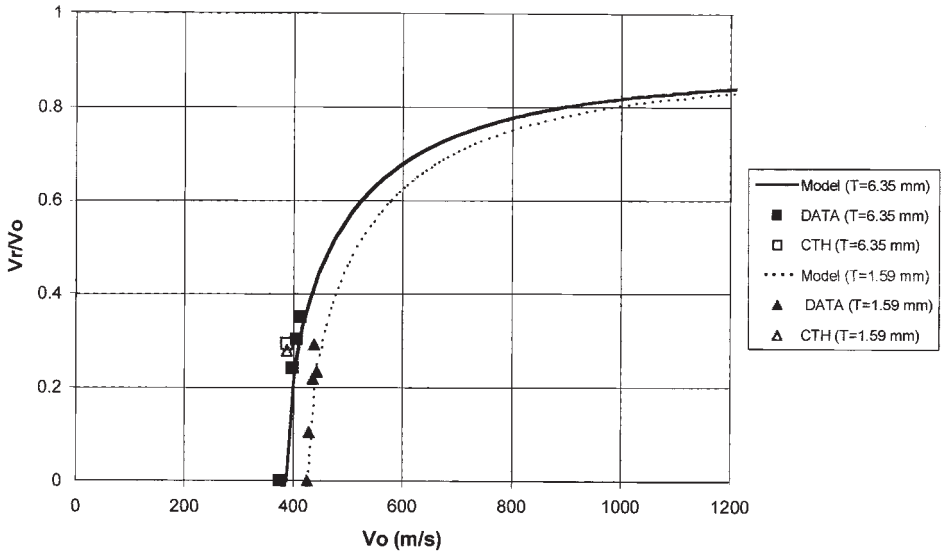

Figure 6: Normalized residual velocity predictions compared with test results for the 12.7 mm and 1.59 mm spheres impacting aluminium plates (T/D=0.5)

CONCLUSIONS

The ballistic limit velocity test results for steel spheres presented herein confirm the existence of a size effect wherein V_{50} values for a constant normalized plate thickness increase with decreasing sphere diameter, but the effect is not as dramatic as that indicated by the Mascianica data for steel FSP's. The cylinder data indicate 30–60% increases in V_{50} values as fragment weight falls below 2–3 grains while the V_{50} values for spheres only increase by about 10%. Work-energy considerations indicate that observed increases in the plate plug diameter to sphere diameter ratio with decreasing size scale could account for the size effect for the spheres. The CTH numerical simulations do not predict the increase in the plate plug diameter ratio with decreasing size scale. The CTH results further indicate that the current strain rate dependencies incorporated in the Johnson-Cook strength and fracture models only account for a 5% increase in the residual velocities and a 1% increase in estimated V_{50} values with an 8-fold decrease in sphere size. It is possible that the remainder of the size effect derives from less damage accumulation (e.g., void growth) in the plates over the shorter penetration times associated with the smaller size scales [3]. A time dependent damage model might also account for the growth in the relative plate plug diameter and also explain why cylinders, with higher plate shear strain gradients, experience a larger size effect than the spheres.

It is recommended that a similar series of ballistic limit velocity tests be performed with steel cylinders and aluminum target plates with measured hardness values to confirm the size effect evident in the Mascianica FSP data and that both the sphere and cylinder target plates be sectioned and examined microscopically for variations in microscopic damage accumulation with decreasing size scale.

REFERENCES

1. Yatteau, J.D., K.T. Edquist, and R.H. Zernow, "Penetration Model Assessment for Small Fragments", Applied Research Associates, Inc., 5941 S. Middlefield Rd., Suite 100, Littleton, C, 80123, for Naval Surface Warfare Center, Dahlgren Division, Dahlgren VA, 22448-5110, February 10, 2000.
2. Mascianica, F.S., "Ballistic Technology of Lightweight Armor – 1981 (U)", U.S. Army Materials Technology Laboratory, AMMRC TR81-20, May, 1981.
3. Anderson, C.E., Private Communication, November, 2000.
4. Bell, R.L., M.R. Baer, R.M. Brannon, M.G. Elrick, E.S. Hertel, S.A. Silling, and P.A. Taylor, "CTH Users Manual and Input Instructions version 4.00", Sandia National Laboratories, Albuquerque, NM, 1998.
5. Recht, Rodney F., "Chapter 7: High Velocity Impact Dynamics: Analytical Modeling of Plate Penetration Dynamics," *High Velocity Impact Dynamics*, edited by Jonas A. Zukas, pp. 443–514, 1990.